Where Quantum and Fluids entangle

Quantum Computational Fluid Dynamics
Core Tensor Network QCFD Set
Project number 101080085

Call:	HORIZON-CL4-2021-DIGITAL-EMERGING-02
Topic:	HORIZON-CL4-2021-DIGITAL-EMERGING-02-10
Type of action:	HORIZON Research and Innovation Actions
Granting authority:	European Commission-EU
Project starting date: fixed date:	1 November 2022
Project end date:	31 October 2026
EU-Project duration:	48 months
Project Coordinator:	University of Hamburg (UHH)
Work Package Leader	University of Hamburg (UHH)
Cooperations	Technical University of Crete (TUC), PlanQC
Deliverable number:	D4.1
WP contributing to the deliverable:	WP#4 Tensor Network Simulations
Deliverable Type:	Data
Revision:	0
Dissemination level:	Public
Due Submission date:	28.06.2024
Prepared By:	UHH, TUC, PlanQC
Internal Reviewers:	DJ, DA, MK
Final Approval:	DJ

This project receives funding from the European Union's Horizon 2020 HORIZON Research and Innovation Actions Programme under Grant Agreement #101080085

Revision History

Version	Date	Who	Changes
R0	28.06.2024	NH	

Executive Summary

The Quantum Computational Fluid Dynamics (QCFD) project is dedicated to establishing an open-access quantum software framework to address Computational Fluid Dynamics (CFD) challenges present in today's industry.

As a part of the Work Package 4 (WP4) "Tensor Network simulations", Deliverable D4.1: provides a core set of tensor network examples and solutions for comparison with benchmark CFD solutions from work package 1. D4.1 is due in month 21 of the project.

In accordance with the Data Management Plan (DMP), D4.1 follows the FAIR data principles – Findability, Accessibility, Interoperability, and Reusability – where each dataset is provided with a detailed metadata structure with unique identifiers and proper documentation, ensuring that the data is not only easily accessible but also readily transferable and reusable. The access to the public is granted by a dedicated research data repository (FDR) hosted at the university of Hamburg (UHH), https://www.fdr.uni-hamburg.de/communities/qcfd/. To facilitate the users overview, all datasets belonging to the QCFD project will be collected in a QCFD community group on the mentioned data server.

This project receives funding from the European Union's Horizon 2020 HORIZON Research and Innovation Actions Programme under Grant Agreement #101080085

Content

This project receives funding from the European Union's Horizon 2020 HORIZON Research and Innovation Actions Programme under Grant Agreement #101080085

List of abbreviations

Acronym / Short Name	Meaning
CA	Consortium Agreement
CFD	Computational Fluid Dynamics
CFL	Courant-Friedrichs-Levy criteria
D	Deliverable
DMP	Data Management Plan
DOI	Digital Object Identifier
EC	European Commission
ENG	ENGYS SRL
EU	European Union
FD	Finite Difference
FDR	Research Data Repository
FV	Finite Volume
FZL	Jülich Research Centre
KPI	Key Performance Indicator
LES	Large-Eddy Simulation
PlanQc	PlanQc GMBH
PO	Project Officer
QCFD	Quantum Computational Fluid Dynamics
VQA	Variational Quantum Algorithm
TUHH	Technical University of Hamburg
TUC	Technical University of Crete
TUM	Technical University of Munich
UHH	University of Hamburg
WP	Work Package
WPL	Work Package Leader

This project receives funding from the European Union's Horizon 2020 HORIZON Research and Innovation Actions Programme under Grant Agreement #101080085

1 Introduction

The development of digital computers has enabled Computational Fluid Dynamics (CFD) as an essential tool in modern fluid dynamics research, substituting traditional semi-analytical methods. This advancement has significantly increased efficiency in solving fluid dynamics problems resulting in the expansion of the field to more sophisticated investigations. Similarly, the progress in quantum computers and quantum algorithms offers the potential for another revolutionary transformation in tackling fluid mechanics challenges. Therefore, this deliverable aims to prepare and benchmark quantum-inspired methods for CFD problems to quantitatively assess their potential.

The data aims to assess the quality, accuracy and efficiency of tensor network methods, which can readily be converted into quantum algorithms, by applying them to problems that have been identified in WP1 and WP2 of the project. These results are often directly comparable to classical CFD methods which are also provided, where appropriate. To this end, a representative selection of core tensor network cases is designed and provided in this deliverable, ensuring its scientific and industrial relevance.

Dataset-specific documentation to support the interpretation and outline the usability of the data is given. Furthermore, the datasets are accompanied by metadata, including parameters, software versions, library dependencies, and simulation time frames. Lastly, the data sets are enhanced by a keyword-based search system incorporating Digital Object Identifiers (DOIs). With this documentation process, we intend to guarantee the replication of our (and other) methods and promote accessibility to the scientific and industrial sectors.

The complete data is made available, according to the submitted Data Management strategy, in a dedicated research data repository (FDR) hosted at the University of Hamburg (UHH), www.fdr.uni-hamburg.de/communities/qcfd/, and associated within the project community QCFD.

2 Fundamentals of Data Description

We follow the same process and notation as for deliverable D1.1 and provide its description here again. We define the fundamental data processing pipeline, the quality/accuracy requirements, and the performance indicators, e.g., fail/pass criteria. This section's scope is to secure data quality.

The overall goal of QCFD is to combine the computational resources of quantum hardware with CFD industrial applications. To this end, established CFD tools, that have proven to display good agreement with the underlying physical phenomena, are used as benchmark (verification) examples for the algorithmic transition from classical to the quantum frameworks.

To highlight the application relevance, the document distinguishes between scientific and industrial motivation. Each example case holds a simplified categorization which transits between industrial and scientific relevance, cf. Figure 1.

FIGURE 1: APPLICATION INDICATOR SLIDER

2.1 Accuracy

Data accuracy is fundamental for expressive and trustful benchmarking and is therefore also a key aspect of this deliverable D1.1. In this regard, the employed guidelines are given next:

- List of file formats with the corresponding accuracy, accessible without compression
  - Fortran std file format
  - .hdf5
  - .csv

This project receives funding from the European Union's Horizon 2020 HORIZON Research and Innovation Actions Programme under Grant Agreement #101080085

- Double-precision floating-point number format
- For complex numbers, the 53-bit significant precision of 16 decimal digits is divided between real and imaginary parts.

2.2 Assessment Criteria

- Absolute Error: Measure of the deviation between two paired variables.
- L2-(or Euclidean) Norm: In general, a norm consists of a function mapping from a vector space to a non-negative real number. In particular, the L2-norm is defined as the square root of the scalar product of a vector with itself.
- Fidelity: Often understood as a similarity measure and formed by the scalar product of two normalized vectors.
- Trace Distance: Measure of how distinguishable two (quantum) states are. For pure quantum states, the trace distance is defined as the square root of one minus fidelity, i.e. the square root of the difference between one and the fidelity.

3 Cases

This section contains a complete set of core CFD problems investigated using tensor networks and constitutes the QCFD deliverable D4.1. Considering the landscape of CFD problems and to cover different branches of the (Q)CFD, we have chosen several cases as representative of each branch to be tested by our tensor networks methods. We have categorized these problems based on the spatial dimensions of the selected problem. Therefore, we have 1D (textbook) cases and 2D problems. Each category is split into subsections containing different benchmarks which are uniquely identified by an individual DOI.

In what follows, we have neglected the flow compressibility since Mach numbers are small, $\mathrm{Ma} < 0.1$, where the Mach number $\mathrm{Ma} = u/a$ corresponds to the ratio between flow speed u and the speed of sound a. We have used non-dimensional parameters for our studies, in particular the Reynolds number

$$Re = uL/\nu = \frac{\text{inertial force}}{\text{viscous force}}$$

where u is the characteristic velocity, L the characteristic length, ν the viscosity.

The Nusselt number

$$Nu = \frac{hL}{k} = \frac{\text{convective heat transfer}}{\text{conductive heat transfer}}$$

where h is the heat transfer coefficient, L is the characteristic length, and k is the thermal conductivity.

The Peclet number is defined as

$$Pe = \frac{uL}{D} = \frac{\text{advection transport}}{\text{diffusive transport}}.$$

Here, u is again the characteristic velocity, L the characteristic length, and D the diffusivity.

Additionally, the properties of the numerical solver are quantified by the Courant-numbers also known as CFL numbers $C_c = u\Delta t/\Delta x$ for convection and $C_d = \nu\Delta t/\Delta x^2$ for diffusion. Here Δt is a time step and Δx the spatial discretization step. A restriction is imposed using the ratio between the temporal and spatial discretization to obtain stable explicit time marching computations. It should be noted that in what follows, we conduct our studies with different boundary conditions. The boundary settings include the combinations of Dirichlet-Dirichlet, Neumann-Neumann, Dirichlet-Neumann, Robin-Robin, and periodic boundary conditions on the left-right boundary which are given in Table 1.

TABLE 1: BOUNDARY SETTINGS USED IN OUR STUDIES

Boundary Setting	Condition
Dirichlet – Dirichlet	$y(0) = a$ $y(1) = b$
Neumann - Neumann	$\partial y/\partial x \mid_{x=0} = a$ $\partial y/\partial x \mid_{x=1} = b$
Dirichlet - Neumann	$y(0) = a$ $\partial y/\partial x \mid_{x=1} = b$
Robin - Robin	$ay(0) + \partial y/\partial x \mid_{x=0} = c$ $by(1) + \partial y/\partial x \mid_{x=1} = c$
Periodic	$y(0) = y(1)$

3.1 1D Textbook Case: Burgers Equation

Industrial 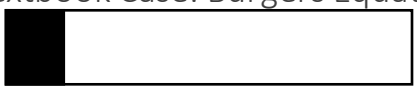 Scientific

This first category refers to 1D textbook cases. Here, we are interested in using the tensor network approach for representing fluid flows in Variational Quantum Algorithms (VQAs) to solve the Burgers equation. In the previous work package deliverable D1.1, we showed VQA methods can be employed to study problems such as Burgers equation which resulted in the publication of two papers namely (Jaksch, Givi, Daley, & Rung, 2023) and (Over, et al., 2024). In what follows, a detailed case description for the corresponding numerical experiments is given in each subsection. Note that the density ρ and the viscosity ν are both set to 1.

The 1D Burgers equation is a non-linear differential equation that considers convective influences, i.e., $Pe \neq 0$. The equation is often used as a simplified model and has applications in areas such as shock waves, turbulence, and traffic flow. The simulation of the 1D Burgers equation with variational quantum algorithms and the study of different ansatz techniques was carried out. All studies employ an initial Dirac velocity distribution $u_{max} = 20\pi\ m/s)$ at $t = 0s$. The evolution over the time horizon from $0 - 4s$ is exemplarily depicted in Figure 2. Simulations were performed within a Master Thesis on Variational quantum algorithms for $Re = u_{max}L/\nu = [200\pi - 20000\pi]$, with the viscosity ν in $[0.1, 0.01, 0.001][m^2/s]$.

This project receives funding from the European Union's Horizon 2020 HORIZON Research and Innovation Actions Programme under Grant Agreement #101080085

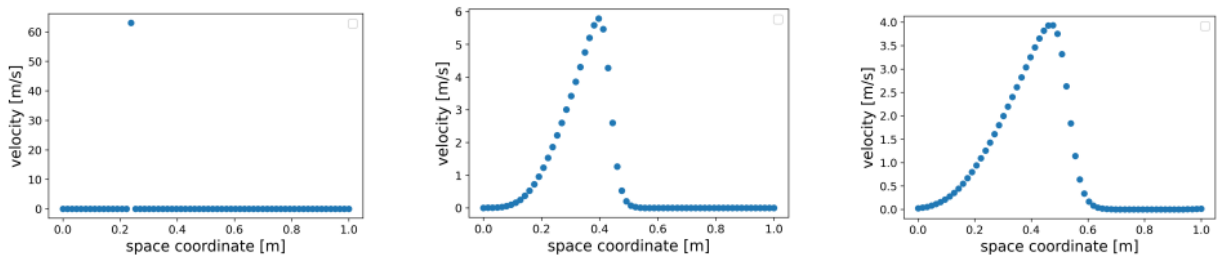

FIGURE 2: RESULTS FOR THE 1D BURGERS EQUATION

To show the translatability of the tensor network approach in variational quantum algorithms, we have produced random MPS with different bond dimensions χ, different ansatzes, and different ansatz depths with variational quantum networks. The behavior of the achieved fidelity between the original MPS state and the quantum state was investigated.

To generate the random MPS, we decomposed random vectors to MPS and truncated the required bond dimension. We observed the expected behavior where the fidelity increases with the number of layers and thus observing the expressibility of the ansatz. We have depicted this for eight qubits and different bond dimensions χ in Figure 2. It should be noted that representing MPS of higher bond dimensions requires deeper ansatzes.

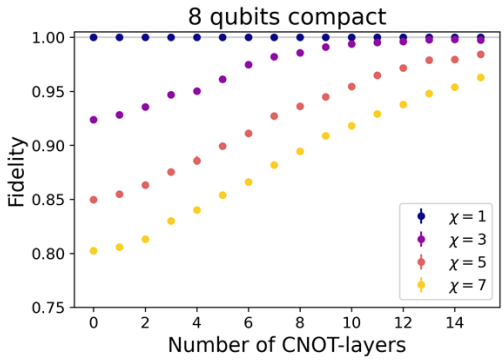

FIGURE 3: RESULTS FOR THE GENERATION OF RANDOM MPS WITH VARIATIONAL QUANTUM NETWORKS. THE FIDELITY INCREASES WITH AN INCREASING NUMBER OF LAYERS AND THUS THE EXPRESSIBILITY OF THE ANSATZES

Furthermore, we investigated the optimum generation of different MPS for each of the different ansatzes. Figure 2 shows how the achievable fidelity for two different ansatzes and two different bond dimensions develops with the number of CNOT layers for 8 qubits. The compact ansatz, which always entangles neighboring qubits, was compared with the shuffle ansatz, which entangles qubits at different distances of powers of 2. It was found that the 'compact' ansatzes represent smaller bond dimensions better and the 'shuffle' ansatz represents higher bond dimensions better. The results are given in Figure 23.

This project receives funding from the European Union's Horizon 2020 HORIZON Research and Innovation Actions Programme under Grant Agreement #101080085

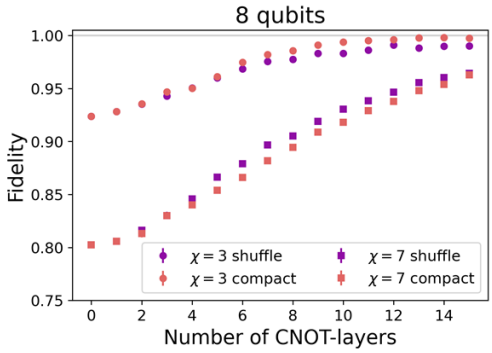

FIGURE 4: COMPARISON OF DIFFERENT ANSATZES FOR GENERATING MPS STATES OF DIFFERENT BOND DIMENSIONS. THE 'COMPACT' ANSATZ REPRESENTS SMALLER BOND DIMENSIONS, AND THE 'SHUFFLE' ANSATZ REPRESENTS HIGHER BOND DIMENSIONS BETTER

Access to the data is provided under DOI 10.25592/uhhfdm.14232.

3.2 2D Problems

In this section, we are concerned with 2D spatial problems and treat them with tensor network algorithms. It includes the propagation of a point source with non-reflective boundaries, simulations of the Lid-driven and Doubly-driven cavity and scalar transport in not-rectangular domains.

3.2.1 2D Point-Source Propagation

Industrial  Scientific

This problem setting is motivated by the need to investigate the noise propagation of an airplane turbine on the environment to estimate the noise levels on surrounding residents. The dynamics is governed by linearized Euler equations for inviscid fluids

$$\begin{aligned}\frac{\partial p}{\partial t} &= -\bar{\rho}c^2\left(\frac{\partial u}{\partial x}+\frac{\partial v}{\partial y}\right)-\bar{u}\frac{\partial p}{\partial x}+f(x,y,t),\\ \frac{\partial u}{\partial t} &= -\frac{1}{\bar{\rho}}\frac{\partial p}{\partial x}-\bar{u}\frac{\partial u}{\partial x},\\ \frac{\partial v}{\partial t} &= -\frac{1}{\bar{\rho}}\frac{\partial p}{\partial y}-\bar{u}\frac{\partial v}{\partial x},\end{aligned}$$

where p is the pressure field fluctuation, u (v) is the velocity field fluctuation component in the x-(y-)direction, $\overline{\rho}$ is the mean density, c is the velocity of source, $\overline{u}$ is the base flow, considered to be only in the x-direction. The source to be studied is a sinusoidal point source. Further, we impose non-reflective boundary conditions. For this purpose, we developed a quantum-inspired analogue of the sponge layers method.

To solve this PDE, we discretize it by means of a staggered grid and finite differences, where spatial derivatives are discretized with second-order accurate central differences. The time integration is done by a Runge-Kutta 4th order scheme. As an example, results for a $256 \times 256 (N_x \times N_y)$(staggered) grid are shown in Figure 4.

The dataset can be found under DOI 10.25592/uhhfdm.14459.

This project receives funding from the European Union's Horizon 2020 HORIZON Research and Innovation Actions Programme under Grant Agreement #101080085

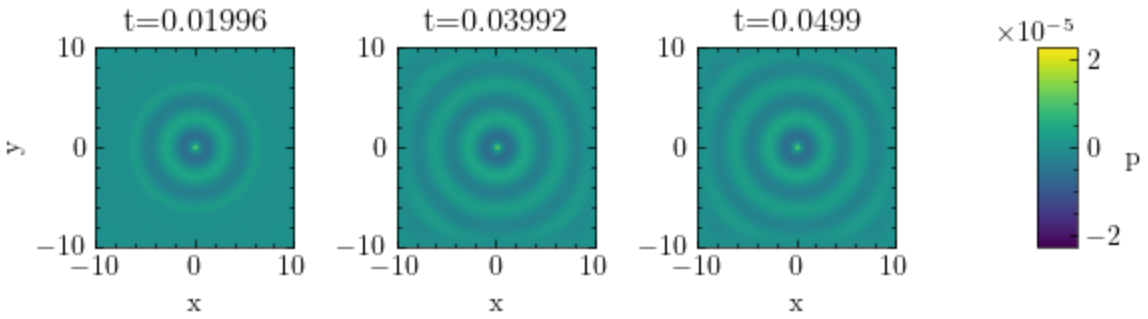

FIGURE 4: RESULTS FOR THE 2D NOISE PROPAGATION WITH POINT-SOURCE AND NO BASE FLOW

To conduct a scaling analysis of our tensor network algorithm for the 2D noise propagation problem, we ran preliminary simulations with different bond dimensions and numbers of qubits. For this purpose, we ran simulations with varying bond dimensions and numbers of qubits n per dimension, measuring the computational time required to complete 100 steps using 4th order Runge-Kutta integration method. To ensure validity, the timer starts as soon as the central tensor reaches the specified maximum permitted bond dimension. Hence, initial steps where the MPS has not yet built up any entanglement are prevented from corrupting the results. Once this condition is met, the computational time should scale with the most expensive operation. The results are shown in Figure 6. We observe that the CPU time, plotted on a logarithmic scale, does not increase linearly with the bond dimension or the grid size. This suggests that an exponential relationship between the CPU time and grid size, as expected in a direct numerical simulation, can be ruled out. Instead, the CPU time appears to exhibit sublinear growth as the maximum permitted bond dimension increases.

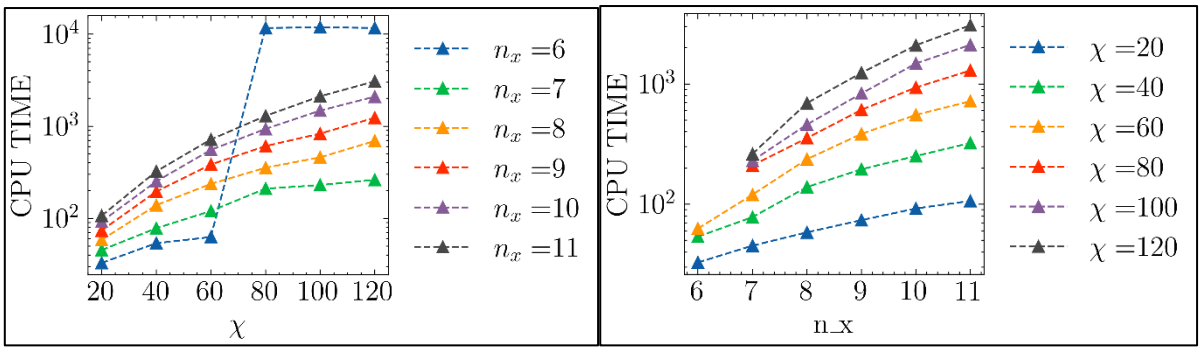

Figure 5: Results for the scaling analysis of the tensor network algorithm on the 2D noise propagation without base flow

3.2.2 Lid-driven and Doubly-Driven Cavity

Industrial  Scientific

The setup for the lid-driven cavity in two spatial dimensions is shown in Figure 6. We consider a square box with edge length L, and the upper lid moves with velocity u_0 in x-direction. The x-component (y-component) of the fluid is denoted by $u(v)$. At $t = 0s$, the fluid is at rest, $u = v = 0\ m/s$. We consider a viscous fluid with kinematic

viscosity ν and seek solutions to the incompressible Navier-Stokes equations in the stream-function-vorticity approach.

We scale time in units of $t_0 = L/u_0$, length in terms of L and velocities by u_0. Solutions to the Navier-Stokes equations are then characterized by the Reynolds number $Re = u_0 L/\nu$. We discretize the interior of the cavity (excluding boundaries) by a uniform grid with K grid points in each spatial dimension. The computational domain thus comprises K^2 equally spaced points with grid spacing $h = L/(K+1)$. The boundary conditions for u, v, and the stream function ψ and for the lid-driven cavity are shown in Figure 6(b). In the case of the doubly-driven cavity, the upper lid continues to move at constant velocity u_0 in the x-direction. In addition, the bottom lid moves at a constant velocity -u_0 in the x direction. The corresponding boundary conditions are specified in Figure 6(c).

We introduce a tensor network algorithm for solving the lid-driven and doubly-driven cavities in (Kiffner & Jaksch, 2023). We represent the velocity components by matrix product states and find that the bond dimension grows logarithmically with simulation time. The tensor network algorithm requires at most a few percent of the number of variables parametrizing the solution obtained by direct numerical simulation, and approximately improves the runtime by an order of magnitude compared to direct numerical simulation on similar hardware.

In (Kiffner & Jaksch, 2023), we present a general framework for dealing with typical CFD boundary conditions in a tensor network approach. This includes a strategy for dealing with ghost points at the boundaries and the development of matrix product operators adapted to moving and fixed walls. In this way, we show that the tensor network approach can be generalized to more complex flow geometries.

The dataset can be accessed via DOI 10.25592/uhhfdm.14236.

(a)

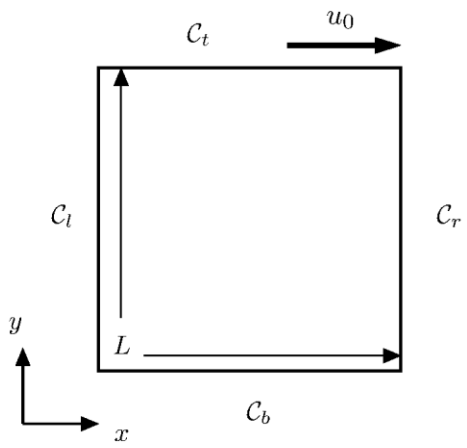

(b)

	$\mathcal{C}_t$	$\mathcal{C}_r$	$\mathcal{C}_b$	$\mathcal{C}_l$
u	u_0	0	0	0
v	0	0	0	0
ψ	0	0	0	0

(c)

	$\mathcal{C}_t$	$\mathcal{C}_r$	$\mathcal{C}_b$	$\mathcal{C}_l$
u	u_0	0	$-u_0$	0
v	0	0	0	0
ψ	0	0	0	0

FIGURE 6: LID-DRIVEN AND DOUBLY-DRIVEN CAVITY

3.2.3 Scalar Transport in Non-Rectangular Domains

Industrial  Scientific

In the following, we study transport in non-rectangular domains. In the first case, we focus on a passive scalar transport equation $\partial_t \phi = -\vec{u} \cdot \nabla\phi + \Gamma\nabla^2\phi$ for a fixed velocity $\vec{u} = 0.5[\cos(\alpha), \sin(\alpha)]^T [m/s]$. The angle α of the velocity is chosen to be [0°,45°,90°,140°]. The Reynolds number in the computational domain reads $Re = uL/\Gamma = 2000\pi$, based on the length $L = 2\pi$ of the (computational) domain, the velocity magnitude $u = 0.5\ [m/s]$ and a

constant diffusion coefficient $\Gamma = 0.002$. We employ a tensor network representation for the differential operators, along with a corresponding relation to capture the metric terms between physical (non-rectangular) and computational (rectangular) domain. The computational domain is a square $\xi \in [0, L] \times \eta \in [0, L]$, whereby the physical domain is described by $x = \xi - \alpha\, sin(\xi - \eta)$ and $y = \eta - \alpha\, sin(\xi - \eta)$. Discretization of the problem is done by using a central finite differences approximation for all transport derivatives and all metric derivatives on a grid with 64×64 discrete points. It should be noted that discrete points are equidistantly distributed in the computational domain. The evolution of the time horizon takes place from$0s$ to $10s$. We use constant time steps of $\Delta t = 0.05s$ alongside of a first-order explicit scheme conserving a Courant Number of C_c=1.0 to discretize time derivatives. We investigate the evolution of an initial Gaussian pulse

$$\phi(x, t_0) = A \exp\left(\frac{(x - x_0)^2 + (y - y_0)^2}{B}\right)$$

with $A = 1.0, B = 0.2$, and $x_0 = \pi, y_0 = \pi$, propagating in a physical domain with periodic boundary conditions. The results of the simulation with the prescribed velocity at $\alpha = 140°$ is given in Figure .

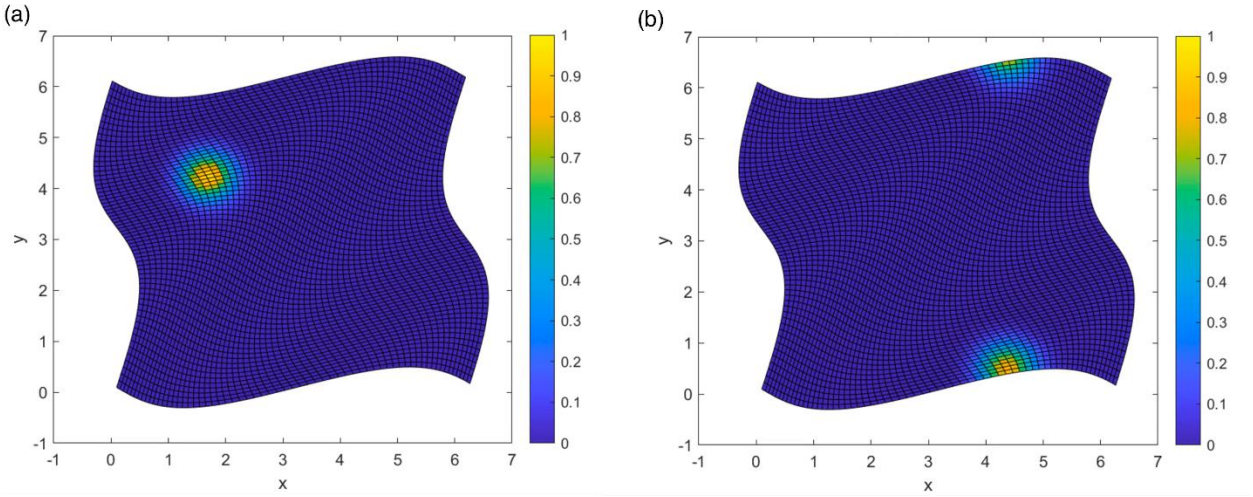

FIGURE 8: SNAPSHOTS OF THE SCALAR FIELD FOR THE GAUSSIAN PULSE EVOLUTION WITH PRESCRIBED VELOCITY AT $\alpha = 140°$ FOR 0.1S (A) AND 0.3S (B).

Next, Navier Stokes simulations have been used to extend the application of tensor network methods to curvilinear geometries. A fluid viscosity $\nu = 0.001 m^2/s$ was employed for the simulation and using Large-Eddy Simulations (LES) and a Smagorinsky model, a spatially variable viscosity was obtained ($c_s = 0.15$). The pressure was computed via solving an additional Poisson equation with a pressure projection approach. The physical domain is the same as in the case described in Figure . The time horizon spans 0s to $10s$ which is discretized using an explicit 4th order Runge-Kutta scheme. We restrict the dynamic time step to maintain a small Courant number well below 1. The periodic boundary conditions in the horizontal-direction and zero Dirichlet boundary conditions in the vertical-direction were used for the simulation. A parabolic horizontal velocity profile along the η-axis of the domain was considered as an initial condition. The maximum initial velocity u_{max} was obtained at the channel centerline, given by the profile $u(\eta) = -1/\pi^2 \eta\,(\eta - 2\pi)$. The corresponding similarity parameter was obtained as $u_{max} L/\nu \approx 6200$. For the ζ-component of the velocity $v(\eta, \zeta)$, zero initial velocity is considered. Figure 7 displays the results of the study for the velocity (a), pressure (b) and the divergence of the velocity (c).

The related data to the simulation can be found in DOI 10.25592/uhhfdm.14264.

This project receives funding from the European Union's Horizon 2020 HORIZON Research and Innovation Actions Programme under Grant Agreement #101080085

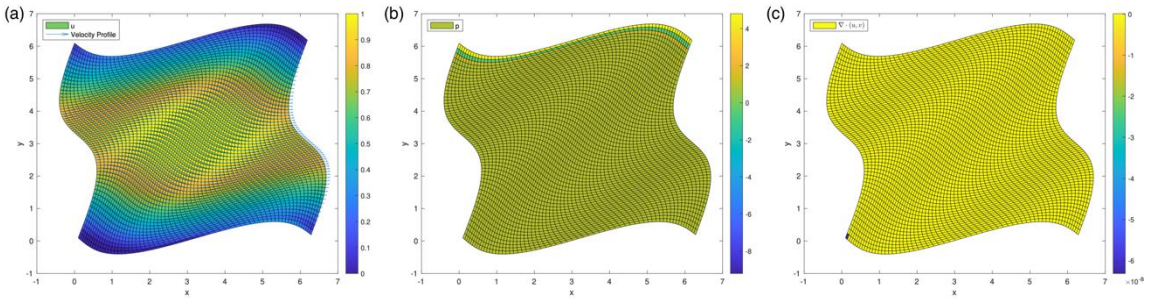

FIGURE 7: VELOCITY PROFILE, PRESSURE AND DIVERGENCE OF THE VELOCITY

References

Jaksch, D., Givi, P., Daley, A. J., & Rung, T. (2023). Variational Quantum Algorithms for Computational Fluid Dynamics. *AIAA Journal, 61*, 1885-1894. doi:10.2514/1.J062426

Over, P., Bengoechea, S., Rung, T., Clerici, F., Scandurra, L., de Villiers, E., & Jaksch, D. (2024). Boundary Treatment for Variational Quantum Simulations of Partial Differential Equations on Quantum Computers. *Preprint on arXiv*. doi:10.48550/arXiv.2402.18619

Kiffner, M., & Jaksch, D. (2023). Tensor network reduced order models for wall-bounded flows. *Physical Review Fluids, 8*, 124101. doi:10.1103/physrevfluids.8.124101